Nuclear Instruments and Methods in Physics Research B 369 (2016) 98–102

Contents lists available at ScienceDirect

Nuclear Instruments and Methods in Physics Research B

journal homepage: www.elsevier.com/locate/nimb

Wannier threshold theory for the description of the two-electron cusp in the ion-induced double ionization of atoms

R.O. Barrachina [a,*], L. Gulyás [b], L. Sarkadi [b]

[a] Centro Atómico Bariloche and Instituto Balseiro, Comisíon Nacional de Energía Atómica and Universidad Nacional de Cuyo, 8400 Bariloche, Río Negro, Argentina
[b] Institute for Nuclear Research of the Hungarian Academy of Sciences (ATOMKI), Pf. 51, H-4001 Debrecen, Hungary

ARTICLE INFO

Article history:
Received 18 June 2015
Received in revised form 19 September 2015
Accepted 22 September 2015

Keywords:
Electron correlation
Electron cusp
Threshold laws
Wannier theory

ABSTRACT

The double electron capture into the continuum states of the projectile (double ECC) is investigated theoretically in collisions of 100 keV He^{2+} ions with He atoms. The process is described within the framework of the impact parameter and frozen-correlation approximations where the single-electron events are treated by the continuum distorted wave method. On the other hand, the Wannier theory is employed for describing the angular correlation between both ejected electrons. This treatment substantially improved the agreement between the theory and experiment as compared to the previous version of the theory (Gulyás et al., 2010) in which the correlation between the ejected electrons was taken into account by the Coulomb density of states approximation.

1. Introduction

Threshold phenomena have attracted the interest of many researchers dealing with scattering processes since the formulation of the threshold laws by Wigner in 1948 [1]. One of the reasons for this interest is explained by the universality of these laws: The energy dependence of the cross section of a collision process in the neighborhood of the threshold energy is governed only by the type of the interaction (long- or short-range, attractive or repulsive), and it is not influenced by the detailed dynamics of the collision.

In the field of energetic ion-atom collisions a unique possibility to study the threshold behavior is provided by the so-called cusp phenomenon. The cusp is a peak appearing in the energy spectrum of the electrons emitted from the collision in the forward direction. The electrons contributing to the cusp move with velocities approximately equal to that of the bombarding ion (atom), i.e., they fly with very small velocities relative to the projectile. By electron spectroscopic measurements of the cusp one can obtain information about extremely low-energy (∼meV) electron emission. This property is due to the kinematic amplification of the electron energies when transformed from the projectile-centered reference system to the laboratory frame. The cusp is regarded as a threshold phenomenon because the final relative electron-projectile energy is just above the ionization limit. A negative relative energy would produce the population of the bound states of the projectile ion. Due to the dominant role of the electron-projectile interaction, the cusp formation is governed by two-body threshold laws. The study of the cusp with different projectiles makes it possible to obtain information about the threshold laws for various types of interactions (Coulomb, dipolar, short-range, see, e.g., Refs. [2–7]).

In the exploration of the threshold character of the cusp, an important step was the experiment by Sarkadi and Orbán [8] in which the two-electron cusp, i.e., the simultaneous emission of two electrons in the forward direction with velocities equal to that of the projectile, was observed. The experiment was carried out for 100 keV He^0 + He collisions. The energies of the electrons resulting from the mutual ionization of the target and the projectile were measured by detecting the triple coincidence between the electrons and the outgoing He^+ ion. A strong correlation between the electron energies in the vicinity of the cusp was observed, which on its turn could be explained by an angular correlation of 180° in the projectile frame [8].

In the final state characterizing the two-electron cusp, the two electrons move slowly relative to the projectile ion. A similar final state consisting of two electrons and an ion occurs in the double photoionization or the electron-impact single ionization of an atom. In 1953 Wannier [9] showed for the first time that the threshold break-up of this three-body system is a highly correlated process, in which the electrons tend to move symmetrically in opposite directions. Since Wannier's pioneering work the

* Corresponding author.
E-mail address: barra@cab.cnea.gov.ar (R.O. Barrachina).

http://dx.doi.org/10.1016/j.nimb.2015.09.070
0168-583X/

correlation between two low-energy electrons in the field of an ion has been the subject of numerous experimental and theoretical studies (see Refs. [10,11] for a review).

In their analysis of the experimental data obtained for the two-electron cusp, Sarkadi and Orbán carried out a Monte Carlo simulation [8,12], in which the correlated motion of the electrons was taken into account according to the Wannier theory. From the simulation they concluded that the prediction of the latter theory was consistent with the observed correlation.

The question of the existence of the two-electron cusp was further investigated by Gulyás et al. [13]. For the description of the double ionization of He by He^{2+} impact they employed the impact parameter and frozen-correlation approximations. Furthermore, in order to better describe the electron–electron correlation, they modified the corresponding Coulomb normalization factor by means of a dynamically screened effective charge. The calculations showed the existence of the two-electron cusp. However, the model described the observed correlation only qualitatively.

The aim of the present work is to improve this model by applying a correlation function that is better suited for the description of the threshold behavior of the two-electron emission. The Monte Carlo simulations performed by Sarkadi et al. [8,12] indicate that the Wannier theory correctly gives account of the angular correlation of the electrons at threshold, therefore in the derivation of the correlation function we rely on this latter theory.

2. Hyperspherical coordinates

Let us consider two electrons in the field of an ion of charge Z_P. The potential reads,

$$V = -Z_P\left(\frac{1}{r_1}+\frac{1}{r_2}\right)+\frac{1}{r_{12}}, \tag{1}$$

with $\mathbf{r}_{12} = \mathbf{r}_1 - \mathbf{r}_2$. Here $\mathbf{r}_1$ and $\mathbf{r}_2$ are the positions of the electrons in the reference system centered at the projectile ion. We parametrize these quantities in terms of hyperspherical coordinates [14–16]

$$\begin{aligned} R &= \sqrt{r_1^2+r_2^2},\\ \vartheta &= \arctan\frac{r_2-r_1}{r_2+r_1},\\ \varphi &= \frac{\pi-\arccos(\hat{\mathbf{r}}_1\cdot\hat{\mathbf{r}}_2)}{2}, \end{aligned} \tag{2}$$

so that the potential reads,

$$V = -\frac{Z(\vartheta,\varphi)}{R}, \tag{3}$$

with

$$Z(\vartheta,\varphi) = \frac{2\sqrt{2}Z_P\cos\vartheta}{\cos 2\vartheta} - \frac{1}{\sqrt{1+\cos 2\vartheta\cos 2\varphi}}. \tag{4}$$

3. Wannier mechanism

The key point in the previous rewriting of the potential in terms of ϑ and φ is that while the hyperradius R parametrizes the size of the two-electron system, the angles ϑ and φ characterizes the radial and angular correlations, respectively. As the system expands (i.e. for increasing R) at the energy threshold, the dynamics tends to be dominated by the symmetric escape of both electrons along opposite sides of the ion. This so-called Wannier mechanism is clearly shown by the function Z which has a saddle point at $\vartheta = \varphi = 0$. Around this point the effective charge Z can be approximated by

$$Z(\vartheta,\varphi) \approx Z_0 + \frac{1}{2}Z_1\,\vartheta^2 + \frac{1}{2}Z_2\,\varphi^2, \tag{5}$$

with $Z_0 = (4Z_P-1)/\sqrt{2}, Z_1 = (12Z_P-1)/\sqrt{2}$ and $Z_2 = -1/\sqrt{2}$. The motion around $\varphi = 0$ (i.e. $r_1 = r_2$) is therefore stable and represents the angular correlation between the electrons, whereas the motion around $\vartheta = 0$ (i.e. $\hat{\mathbf{r}}_1 = -\hat{\mathbf{r}}_2$), which corresponds to the radial correlation, is unstable. For future reference, let us note that around this point,

$$r_{12} \approx \sqrt{2}\,R\left(1-\frac{1}{2}\,\vartheta^2-\frac{1}{2}\,\varphi^2\right). \tag{6}$$

Furthermore, let us note that while the basis of the hyperspherical method lies in replacing the radial distances r_1 and r_2 by the hyperradius R as a measure of the mean size of the system, different authors have employed different sets of pseudo-angles to represent the relative positions of the particles at fixed R [17]. In this context, our particular choice of ϑ and φ leads to a more symmetric representation of the effective charge Z and other related quantities than more commonly employed definitions.

4. Continuum distorted wave theories

Wannier [9] showed that this mechanism, where both electrons escape along opposite sides of the ion, is of the utmost relevance in the threshold limit, *i.e.* at the two electron cusp. However, standard continuum distorted wave (CDW) theories fail to describe this limit correctly. In order to understand the origin of this failure, let us follow Brauner et al. [18] and Briggs and Schmidt [11], and consider the normalization

$$F = \frac{2\pi}{k_{12}}\left(\exp\frac{2\pi}{k_{12}}-1\right)^{-1}, \tag{7}$$

of the electron–electron continuum state. Here $\mathbf{k}_{12} = \mathbf{k}_1 - \mathbf{k}_2$, where $\mathbf{k}_1$ and $\mathbf{k}_2$ are the momenta of the electrons with respect to the projectile. This factor is not the only one responsible for the angular correlation, but it provides the major contribution [11]. In the asymptotic (ballistic) regime (i.e. for $\mathbf{r}_i \propto \mathbf{k}_i$), we resort to Eq. (6) and write, for an equal energy-sharing condition,

$$k_{12} \approx 2\sqrt{E}\left(1-\frac{1}{8}\,(\pi-\theta_{12})^2\right), \tag{8}$$

with $E = ({k_1}^2+k_2^2)/2$and $\theta_{12} = \arccos(\hat{\mathbf{k}}_1\cdot\hat{\mathbf{k}}_2)$. Therefore, in the threshold limit (i.e. for $E\to 0$) we can write [11],

$$F \approx \frac{\pi}{\sqrt{E}}\,e^{-\pi/\sqrt{E}}\exp\left(-\frac{\pi}{8\sqrt{E}}\,(\pi-\theta_{12})^2\right), \tag{9}$$

As it was pointed out by Brauner et al. [18], while the gaussian dependence on $\pi-\theta_{12}$ is in concordance with Wannier theory, the remaining factor $\exp(-\pi/\sqrt{E})$ produces a exponential decrease in the threshold limit, even if the electrons were moving in opposite directions.

Following a proposal by Ward and Macek [19], Otranto and Garibotti [20] introduced a multiplicative energy-dependent parameter in the electron–electron coordinate in order to compensate this effect, and applied this theory to the study of photo double ionization processes. Even though this technique represents a clear improvement over standard models, it did not manage to fully compensate the exponential decrease at threshold.

5. Coulomb density of states approximation

In 2010 Gulyás *el al.* [13] proposed a method to improve the performance of the CDW theory at the two-electron cusp. In the framework of the Coulomb density of states (CDS) approximation,

they assumed that the double ionization cross section could be well expressed by the factorization

$$\frac{d\sigma}{d\mathbf{p}_1 d\mathbf{p}_2} = F(\mathbf{k}_1, \mathbf{k}_2) \times \frac{d\sigma^{\rm IPM}}{d\mathbf{p}_1 d\mathbf{p}_2}, \tag{10}$$

where $d\sigma^{\rm IPM}/d\mathbf{p}_1 d\mathbf{p}_2$ was calculated in the independent particle model (IPM) using the CDW method. Here, $\mathbf{p}_i = \mathbf{k}_i + \mathbf{v}_P$ are the momenta of each electron with respect to the residual target ion. In order to improve the description of the electron–electron correlation in the continuum state, a dynamically screened effective charge was incorporated in the corresponding Coulomb normalization factor, namely

$$F(\mathbf{k}_1, \mathbf{k}_2) = \frac{2\pi Z_{12}}{k_{12}} \left(\exp \frac{2\pi Z_{12}}{k_{12}} - 1 \right)^{-1}, \tag{11}$$

with

$$Z_{12} = 1 - \frac{k_{12}^2}{(k_1 + k_2)^2}. \tag{12}$$

This methodology of including a momentum-dependent charge was employed, for instance, by Peterkop [21] in 1962 and by Rudge and Seaton [14] in 1965, and by many other authors thereafter (see references in [13]). By replacing 8 in 12, we can approximate $Z_{12} \approx (\pi - \theta_{12})^2/4$, and therefore

$$F(\mathbf{k}_1, \mathbf{k}_2) \approx \frac{\pi}{4\sqrt{E}} (\pi - \theta_{12})^2 \times \exp\left(-\frac{\pi}{4\sqrt{E}} (\pi - \theta_{12})^2 \right), \tag{13}$$

It is clearly seen that, even though this correction succeeds in incorporating some extra correlation on the angle θ_{12}, now the normalization factor incorrectly vanishes for $\theta_{12} = \pi$ at all energies E.

6. Wannier theory revisited

Let us analyze the physical origin of the gaussian distribution in Eqs. (9) and (13). To this end, we write the corresponding wave function as

$$\psi_{12} = \exp(iS), \tag{14}$$

and assume that the complex action function S verifies the Hamilton–Jacobi equation,

$$(\nabla_1 S)^2 + (\nabla_2 S)^2 = 2(E - V), \tag{15}$$

which, in terms of the hyperspherical coordinates, reads

$$\left(\frac{\partial S}{\partial R}\right)^2 + \frac{1}{R^2}\left(\frac{\partial S}{\partial \vartheta}\right)^2 + \frac{1}{R^2 \cos^2 2\vartheta}\left(\frac{\partial S}{\partial \varphi}\right)^2 = 2E + 2\frac{Z(\vartheta, \varphi)}{R}. \tag{16}$$

Now we follow the usual approach [22,23] and expand the phase S in the hyperspherical coordinates up to the same order than the effective charge in Eq. (5) in the vicinity of the saddle point $\vartheta = \varphi = 0$, namely

$$S \approx \mu_0(R) + \frac{1}{2}\mu_1(R)\,\vartheta^2 + \frac{1}{2}\mu_2(R)\,\varphi^2. \tag{17}$$

Upon substituting in Eq. (16), we obtain at the lowest order in the energy, the following set of independent equations

$$\frac{d\mu_o}{dR} = \sqrt{\frac{2Z_o}{R}} \tag{18}$$

$$\sqrt{\frac{2Z_0}{R}}\,\frac{d\mu_n}{dR} = \frac{Z_n}{R} - \frac{\mu_n^2}{R^2} \tag{19}$$

with $n = 1$ or 2. Their solutions read

$$\mu_0 = 2\sqrt{2Z_0 R} \tag{20}$$

$$\mu_n = \frac{\mu_0}{8}\left(\sqrt{1 + 8\frac{Z_n}{Z_o}} - 1 \right), \tag{21}$$

so that,

$$\mu_0 = 2\sqrt{2(4Z_P - 1)R/\sqrt{2}}, \tag{22}$$

$$\mu_1 = \frac{\mu_0}{8}\left(\sqrt{\frac{100Z_P - 9}{4Z_P - 1}} - 1 \right),$$

$$\mu_2 = \frac{\mu_0}{8}\left(\sqrt{\frac{4Z_P - 9}{4Z_P - 1}} - 1 \right).$$

Note that for $Z_P \leqslant 2$, the parameter μ_2 has an imaginary part. This leads to an exponentially decreasing solution for $R \to \infty$, which produces a contribution to the probability,

$$\begin{aligned} F \propto |\Psi|^2 &= \exp\left[-\mathrm{Im}(\mu_2)\,\varphi^2 \right] \\ &= \exp\left[-\tfrac{1}{4}\sqrt{\tfrac{2(9-4Z_P)R}{\sqrt{2}}}\,\varphi^2 \right]. \end{aligned} \tag{23}$$

In the asymptotic (ballistic) regime, at the limit of zero total energy, $Z_o/R \approx E$ and $\varphi \approx (\pi - \theta_{12})/2$. Therefore,

$$F \propto \exp\left[-\frac{1}{16}\sqrt{\frac{(9 - 4Z_P)(4Z_P - 1)}{E}}(\pi - \theta_{12})^2 \right],$$

In the followings we consider the case $Z_P = 1$ (the justification of this choice is given later) that yields

$$F \propto \exp\left[-\frac{1}{16}\sqrt{\frac{15}{E}}(\pi - \theta_{12})^2 \right]. \tag{24}$$

This distribution has a similar gaussian shape as the one analyzed in a previous section, namely

$$F \propto \exp\left[-4\ln 2\,\frac{(\pi - \theta_{12})^2}{\Delta(E)^2} \right]. \tag{25}$$

but with a different half-width at half maximum (HWHM). Here, $\Delta(E) \approx 3.38\,E^{1/4}$; while from Eq. (9) we obtain $\Delta(E) \approx 2.66\,E^{1/4}$. Many other authors (see, for instance, [18,23–34]) have proposed the same gaussian distribution for the angular correlation, and with the same $\Delta(E) = \gamma E^{1/4}$ dependence for the HWHM that is characteristic of the Wannier theory, but with different proportionality factors γ, ranging from 2.66 [11,29] to 3.55 [28]. Departures from the $E^{1/4}$ energy-dependence have also been reported in the literature [35–37].

Let us finally point out that even though some previous models managed to obtain the gaussian shape 25, they also lead to the incorrect vanishing of the cross section for $E \to 0$ or $\theta_{12} \to \pi$, as shown in Eqs. (9) and (13), respectively. Here we have demonstrated that these shortcomings can be avoided by means of a Wannier analysis, without resorting to any ad hoc argument. The same applies to our proposed value for γ, which is derived directly from a Wannier theory, with no need of any extra assumption or data fitting procedure.

7. Results and discussion

Applying the $F(\mathbf{k}_1, \mathbf{k}_2)$ correlation function given by Eq. (24) to $d\sigma^{\rm IPM}/d\mathbf{p}_1 d\mathbf{p}_2$ in Eq. (10), we calculated the energy spectra of the electrons emitted in the forward direction in the double ionization of He by the impact of 100 keV He^{2+} ions. The details of the calculations are given in Ref. [13]. In Fig. 1 we plotted the energy spectra of one of the ejected electrons, say e_1, with the condition that the

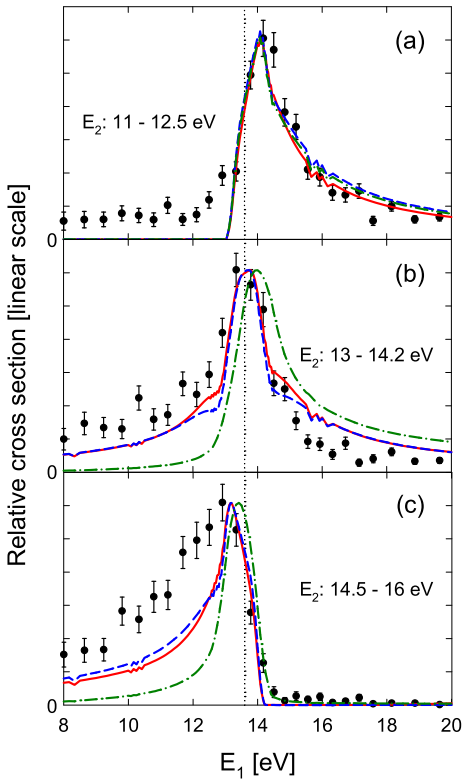

Fig. 1. Energy spectra of the electron e_1 emitted from the process 100 keV $He^{2+} + He \rightarrow He^{2+} + He^{2+} + e_1 + e_2$ with the condition that the energy of e_2 lies in the interval (a) 11–12.5 eV, (b) 13–14.2 eV and (c) 14.5–16 eV. Both electrons are ejected in the forward direction. Full circles: experimental data from the process 100 keV $He^0 + He \rightarrow He^+ + He^+ + e_1 + e_2$ [8]. The solid and dashed line correspond to the present calculations made with $\gamma = 3.38$ and $\gamma = 2.66$, respectively. The dashed-dotted line represents the previous calculations of Gulyás et al. [13].

energy of the other electron, e_2, lies in a narrow range (we may call it "coincidence window"). Panels (a), (b), and (c) correspond to three different coincidence windows. The spectra are normalized at their maxima. We performed the calculations using two different Gaussian widths: $\gamma = 3.38$, as evaluated in the previous section, and $\gamma = 2.66$, which corresponds to the lowest value published in the literature [11,29]. Furthermore, in the figures we have also included the results of the previous calculations by Gulyás et al. [13] that were made with the correlation function expressed by Eqs. (12) and (11). In lack of an experiment for the double ECC process, we compared these theoretical results with the data measured by Sarkadi and Orbán [8]. Although in the experiment the two electrons were emitted in a different process (mutual ionization of the target and the projectile), such a comparison between the theory and experiment can be justified by considering that the main features of the two-electron cusp are dominantly determined by the electron–electron correlation, i.e., the *shape* of the energy distribution of the electrons is expected to be more or less independent from the primary process by which the two electrons are produced. Larger deviations may occur regarding the absolute scale of the cross section, however, the focus of the present work was on the relative cross section. We note that in the experiment the outgoing ion is He^+, i.e., the two low-energy electrons move in the field of a particle of unit positive charge (with respect to the projectile). This justifies the choice $Z_P = 1$ in Eq. (24). Since the electron–electron correlation strongly depends on the asymptotic charge of the projectile, the choice $Z_P = 2$ would lead to results that could not be compared with the experimental data.

According to the figure, the application of the correlation function proposed in the present work substantially improved the agreement between theory and experiment. Its effect is large on the low-energy tail of the cusp for the coincidence conditions defined in panels (b) and (c). However, there is only a small difference between the theoretical curves belonging to the two γ values.

Let us note that the agreement between the theories and the experiment in Fig. 1 is significantly better when the "coincidence window" is below the cusp's energy than when it is above it. The most probable explanation for this effect is related to the post-collisional interaction (PCI) exerted on the electrons by the receding ionized target, as it is discussed in [12]. As is seen in Fig. 1 of [12], the effect is larger for the lower energy electrons, as expected. This PCI effect could be taken into account properly only by means of a four-body treatment of the process.

The Monte Carlo simulation worked out for the two-electron cusp [8,12] confirms this weak dependence of the energy spectra on γ, as we show in Fig. 2. In the simulation, the electron pairs are created randomly in the projectile-centered reference frame with theoretically calculated velocity distribution, and the path of the electrons is tracked until they reach the detectors. As explained in Ref. [12], the main assumptions of this model are that (i) the emission of the electron pairs is isotropic, (ii) the differential cross section for the emission of the electron pair is a linear function, $d\sigma/dE = c_0 + c_1 E$, (iii) The energy E is uniformly shared between the two electrons and (iv) the angular correlation of the electrons is a Gaussian function of width $\gamma E^{1/4}$ peaking at $\theta = \pi$. The c_0/c_1 ratio was varied in order to fit the experimental data,

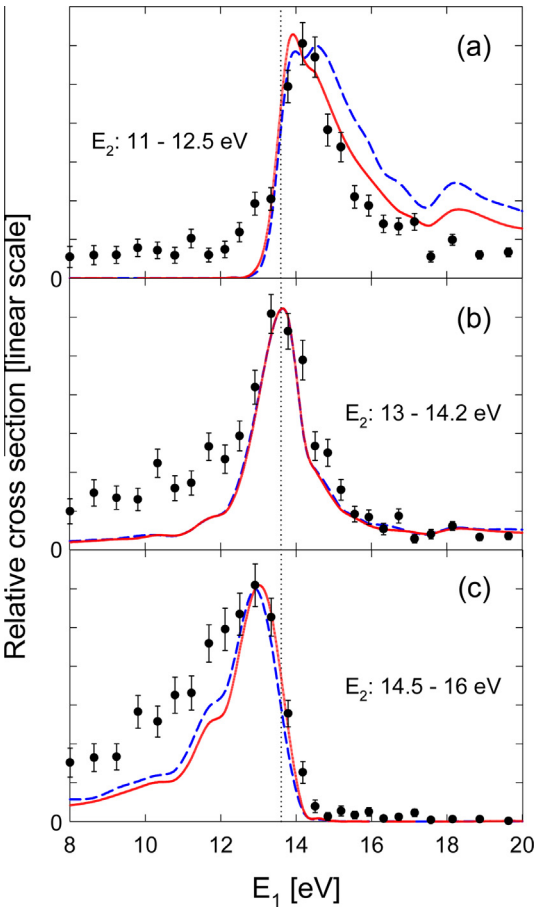

Fig. 2. The same as Fig. 1, but the solid and the dashed line are results of Monte Carlo simulation carried out with $\gamma = 3.38$ and $\gamma = 2.66$, respectively.

resulting $c_0/c_1 = 1.25 \times 10^{-4}$ [8,12] In Fig. 2 this simulation with $\gamma = 2.66$ and 3.38 are compared with the experimental data. The change of γ affects the spectra in a small extent also in this case, although the difference between the curves belonging to $\gamma = 2.66$ and 3.38 is larger than that for the corresponding curves in Fig. 1.

8. Conclusions

In this work we made an attempt to improve the model of Gulyás et al. [13] by applying a correlation function that is better suited for describing the threshold behavior of the two-electron emission. The correlation factor was derived within the WKB approximation, following the approach by Peterkop [22]. With this modified model a substantial improvement was achieved in the theoretical description of the two-electron cusp, as it can be observed in Fig. 1.

In spite of this success, we might note that there is still ample room for improvement in the theoretical description. For instance, our observation that the energy spectra of the electrons depend weakly on the width of Gaussian function describing the angular correlation might be indicating that the width is not so narrow as to make the expansion around the saddle point up to the second order in φ valid [18]. Thus, in spite of the widespread use of Gaussian distributions to represent the angular correlation and the success shown in this and other applications, an improved description is needed [38].

Also from the side of the theory, our model relies on a equal energy sharing emission. This is a basic assumption in most of the models cited in Section 6. However, it might not be well suited for the analysis of the present results. In this sense, a generalization to an unequal energy sharing regime [39] might lead to an improved description of the two-electron cusp.

Furthermore, let us note that the $F(\mathbf{k}_1, \mathbf{k}_2)$ correlation function given by Eq. (24) depends on the *asymptotic* electron momentum. This means that the correlation between the two ejected electrons is included only at infinitely large scattering distances. A further improvement in the theoretical description of the two-electron cusp is expected by applying a correlated two-electron wave function in the transition matrix element, i.e., by a theory that would go beyond the independent particle model (IPM). This theory should give also account of a two-center effect discussed in Ref. [12], namely that the angular correlation between the separating electrons is perturbed by the ionized target.

From the experimental side, more accurate and detailed information about the correlated Wannier state could be obtained by means of the measurements of the two-electron cusp with a considerably improved angular and energy resolution. Furthermore, to make a comparison between theory and experiment for the same collision system and the same reaction process, new experiments and/or further theoretical works are needed.

Acknowledgements

This work was supported by the National Scientific Research Foundation(OTKA, Grant No. K109440), the Universidad Nacional de Cuyo, Argentina (Grant 06/C416) and the Hungarian – Argentinean Intergovernmental S&T MINCYT-NIO Cooperation Programme (Grant No. TÉT_10–1-2011–0100 – HU/10/07). ROB is also a member of the Consejo Nacional de Investigaciones Científicas y Técnicas (CONICET), Argentina.

References

[1] E.P. Wigner, Phys. Rev. 73 (1948) 1002.
[2] Á. Kövér, L. Sarkadi, J. Pálinkás, D. Berényi, Gy. Szabó, T. Vajnai, O. Heil, K.-O. Groeneveld, J. Gibbons, I.A. Sellin, J. Phys. B 22 (1989) 1595.
[3] L. Sarkadi, J. Pálinkás, Á. Kövér, D. Berényi, T. Vajnai, Phys. Rev. Lett. 62 (1989) 527.
[4] F. Penent, J.P. Grouard, J.L. Montmagnon, R.I. Hall, J. Phys. B 25 (1992) 2831.
[5] L. Víkor, L. Sarkadi, Phys. Rev. A 55 (1997) R2519.
[6] R.O. Barrachina, P. Macri, Few-Body Syst. 34 (2004) 175.
[7] L. Sarkadi, R.O. Barrachina, P. Macri, J. Phys. Conf. Series 58 (2007) 219.
[8] L. Sarkadi, A. Orbán, Phys. Rev. Lett. 100 (2008) 133201.
[9] G.H. Wannier, Phys. Rev. 90 (1953) 817.
[10] H.R. Sadeghpour, J.L. Bohn, M.J. Cavagnero, B.D. Esryk, I.I. Fabrikant, J.H. Macek, A.R.P. Rau, J. Phys. B 33 (2000) R93.
[11] J.S. Briggs, V. Schmidt, J. Phys. B 33 (2000) R1.
[12] L. Sarkadi, A. Orbán, Nucl. Instr. Meth. B 267 (2009) 270.
[13] L. Gulyás, L. Sarkadi, A. Igarashi, T. Kirchner, Phys. Rev. A 82 (2010) 032705.
[14] M.R.H. Rudge, M.J. Seaton, Proc. Roy. Soc. Lond. A 283 (1965) 262.
[15] J.H. Macek, J. Phys. B 1 (1968) 831.
[16] C.D. Lin, Phys. Rep. 257 (1995) 1.
[17] S. Watanabe, M. Le Dourneuf, L. Pelamourgues, J. de Physique 43 (1982) C223. C-2.
[18] M. Brauner, J.S. Briggs, H. Klar, J.T. Broad, T. Rösel, K. Jung, H. Ehrhardt, J. Phys. B 24 (1991) 657.
[19] S.J. Ward, J.H. Macek, Phys. Rev. A 49 (1994) 1049.
[20] S. Otranto, C.R. Garibotti, Eur. Phys. J. D 21 (2002) 285.
[21] R.K. Peterkop, Optics Spectrosc. 13 (1962) 87.
[22] R. Peterkop, J. Phys. B 4 (1971) 513.
[23] A.R.P. Rau, Phys. Rev. A 4 (1971) 207.
[24] A.R.P. Rau, J. Phys. B 9 (1976) L283.
[25] H. Klar, J. Phys. B 14 (1981) 3255.
[26] H. Klar, Z. Phys, A 307 (1982) 75.
[27] J.M. Feagin, J. Phys. B 18 (1984) 2433.
[28] F.H. Read, J. Phys. B 18 (1984) 3965.
[29] P.L. Altick, J. Phys. B 18 (1985) 1841.
[30] D.S.F. Crothers, J. Phys. B 19 (1986) 463.
[31] P. Selles, J. Mazeau, A. Huetz, J. Phys. B 20 (1987) 5183.
[32] P. Selles, J. Mazeau, A. Huetz, J. Phys. B 20 (1987) 5195.
[33] P.L. Bartlett, A.T. Stelbovics, Phys. Rev. Lett. 93 (2004) 233201.
[34] S. Otranto, C.R. Garibotti, Phys. Rev. A 71 (2005) 034703.
[35] A. Huetz, J. Mazeau, Phys. Rev. Lett. 8 (530) (2000) 32.
[36] G. Turri, L. Avaldi, P. Bolognesi, R. Camilloni, M. Coreno, J. Berakdar, A.S. Kheifets, G. Stefani, Phys. Rev. A 65 (2002) 034702.
[37] V.V. Serov, V.L. Derbov, T.A. Sergeeva, S.I. Vinitskii, Phys. Part Nucl. 44 (2013) 757.
[38] A.K. Kazansky, V.N. Ostrovsky, Phys. Rev. A 51 (1995) 3712.
[39] S. Cvejanovic, T.J. Reddish, J. Phys. B 33 (2000) 4691.